Effect of Polypropylene Fibers on Self-Healing and Dynamic Modulus of Elasticity Recovery of Fiber Reinforced Concrete

Adham El-Newihy, Pejman Azarsa, Rishi Gupta and Alireza Biparva

January 2018

fibers

MDPI

Article

Effect of Polypropylene Fibers on Self-Healing and Dynamic Modulus of Elasticity Recovery of Fiber Reinforced Concrete

Adham El-Newihy [1], Pejman Azarsa [1], Rishi Gupta [1,*] and Alireza Biparva [2]

[1] Department of Civil Engineering, Facility for Innovative Materials and Infrastructure Monitoring (FIMIM), University of Victoria, 3800 Finnerty Rd., Victoria, BC V8P 5C2, Canada; elnewihy@uvic.ca (A.E.-N.); pazarsa@uvic.ca (P.A.)

[2] Research and Development Manager, Kryton International Inc., 1645 East Kent Ave N, Vancouver, BC V8P 5C2, Canada; alireza@kryton.com

* Correspondence: guptar@uvic.ca; Tel.: +1-(250)-721-7033

Received: 20 December 2017; Accepted: 12 January 2018; Published: 1 February 2018

Abstract: This study aims to evaluate self-healing properties and recovered dynamic moduli of engineered polypropylene fiber reinforced concrete using non-destructive resonant frequency testing. Two types of polypropylene fibers (0.3% micro and 0.6% macro) and two curing conditions have been investigated: Water curing (at ~25 Celsius) and air curing. The Impact Resonance Method (IRM) has been conducted in both transverse and longitudinal modes on concrete cylinders prior/post crack induction and post healing of cracks. Specimens were pre-cracked at 14 days, obtaining values of crack width in the range of 0.10–0.50 mm. Addition of polypropylene fibers improved the dynamic response of concrete post-cracking by maintaining a fraction of the original resonant frequency and elastic properties. Macro fibers showed better improvement in crack bridging while micro fiber showed a significant recovery of the elastic properties. The results also indicated that air-cured Polypropylene Fiber Reinforced Concrete (PFRC) cylinders produced ~300 Hz lower resonant frequencies when compared to water-cured cylinders. The analyses showed that those specimens with micro fibers exhibited a higher recovery of dynamic elastic moduli.

Keywords: concrete self-healing; dynamic modulus of elasticity; fiber reinforced concrete; Impact Resonance Method; crack

1. Introduction

Concrete structures are prone to cracking during their service life. Cracks can be caused by a variety of factors at different stages of their service life such as plastic and drying shrinkage at early age or freeze/thaw cycles at a long-term stage. There are several approaches that can be utilized to limit cracking, such as employing sufficient number of steel bars or fiber reinforcement by implementing an appropriate mix design. However, still some types of cracks are expected. Developed cracks in the concrete matrix create pathways for aggressive agents, such as chlorides, which endanger the structure's durability and reduce its service life. Hence, it is essential to monitor, control, and repair concrete cracks. Repairing cracks may not always be a feasible task as cracks are not always visible or accessible. As reported, costs related to repairs are also equal to half of the annual construction budget in Europe [1]. In the USA, the annual cost for maintaining existing bridges is around $5.2 billion [2] while in the UK, nearly 45% of the budget allocated for the construction industry is spent for repair and maintenance applications [3]. Besides, indirect costs are associated with concrete crack repair due to loss in production and traffic jam occurrence. Although concrete may be susceptible to cracking, its inherent ability to heal itself to a certain level increases its service-life, thus making this material highly beneficial. This time-dependent phenomenon is called "self-healing" of concrete.

Self-Healing (SH) has a rising significance in engineering. In concrete, there are various SH mechanisms including (1) on-going hydration (2) calcium carbonate ($CaCO_3$) precipitation (3) swelling of cement matrix (4) sedimentation of debris and loose cement particles in presence of water (Figure 1). In young concrete, continued hydration is the dominant healing mechanism because of its fairly high content of un-hydrated cement particles whereas calcite formation ($CaCO_3$) becomes the main mechanism at a later age. Based on the healing mechanisms, approaches to SH in concrete can be classified broadly into two main groups, namely autogenous and autonomous healing [4]. Autogenous crack healing in concrete refers to SH properties resulting from the chemical and/or physical composition of cementitious matrix and is only effective for small crack widths up to 200 µm [4]. On the other hand, autonomous crack healing is associated with artificially triggered mechanisms into the cementitious matrix. Due to a small crack width closure, autogenous healing is not a reliable phenomenon to achieve noticeable healing effects. Hence, in recent years, more attention has been paid to engineered healing concepts.

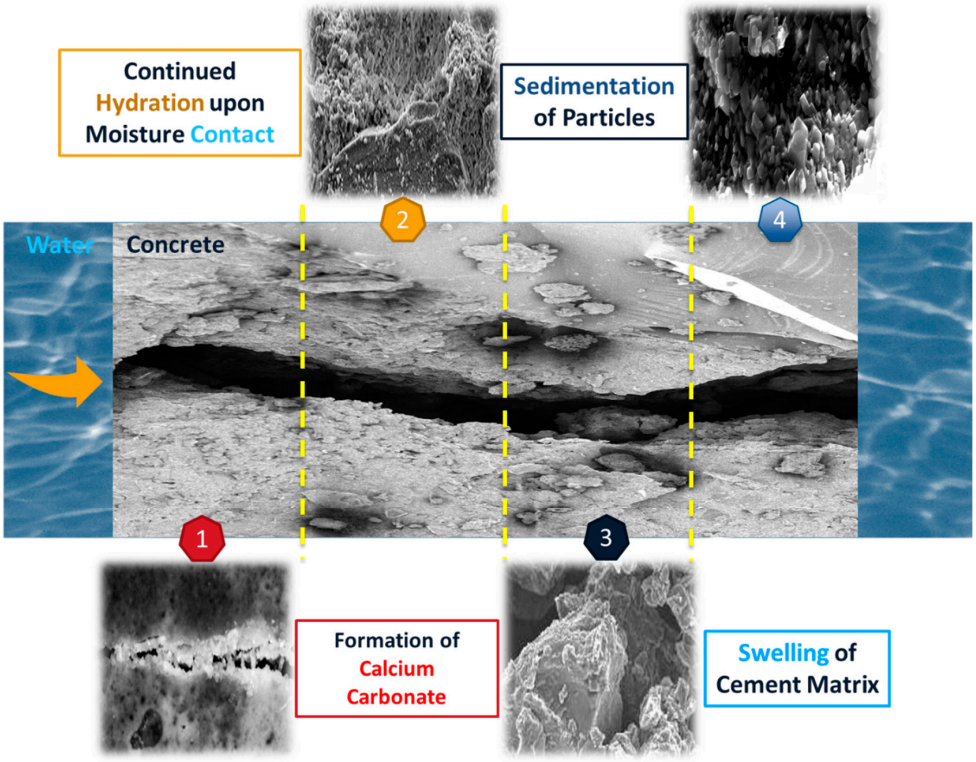

Figure 1. Self-healing mechanisms in concrete.

As a widely known approach to controlling the opening of the cracks, discontinuous and randomly dispersed fibers can be employed in concrete to narrow the crack width and thus provide enough support for any kind of self-healing procedure. When crack occurs in the matrix and as the fibers bridging the cracks start acting, the opening of each single crack will be effectively controlled and restrained due to bridging effect supplied by the fibers. Although the concept of using fibers to reinforce brittle materials has been used for hundreds of years, only few investigations were performed in the past on the self-healing efficiency of ordinary Fiber Reinforced Concrete (FRC) utilizing various types of fibers [5]. Contemporary materials that are commonly used as fibers in concrete include steel, glass, natural (wood, fruit, or grass) or synthetic (polypropylene, nylon and polyester) that have a variety of different shapes and sizes per the required purpose. Although properties of glass fibers improve the concrete composite by increasing the tensile and impact strength, a limitation of using these fibers in concrete is fiber embrittlement due to the high alkalinity of cement binder [6].

Also, metallic fibers such as steel enhance concrete ductility, flexure strength, and fracture toughness; however, they are subjected to the same type of corrosion deterioration as steel reinforcement and thus their durability reduces in high sulfate and chloride exposed environment [7]. Effectiveness of steel and glass fibers depends on adhesive chemical interaction. However, polymer organic fibers such as polypropylene and nylon rely on an interlocking mechanical mechanism and exhibit hydrophobicity, when added to a cementitious medium [8]. The most common type of synthetic fiber reinforcement used in concrete is polypropylene for its high impact resistance, environmental stability, and low production cost. Polypropylene Fiber Reinforced Concrete (PFRC) exhibits a better tensile strength and toughness than regular concrete of the fibers with the matrix. However, the increase in strength is not significant since the fibers have a low modulus of elasticity.

Typical properties that define concrete's structural integrity are its compressive strength and modulus of elasticity. The elastic modulus of concrete is of great interest as a design factor for structures and a reliable condition indicator of in-service structures. It can be determined through the static and dynamic behavior of structural elements. The elastic properties of concrete can be determined using vibration resonance according to American Society for Testing and Materials (ASTM) C215 [9]. The resulting modulus is referred to as the Dynamic modulus of elasticity (E_d). The advantage of using E_d, in monitoring the mechanical properties of concrete over static modulus of elasticity, is that the dynamic modulus is sensitive to changes within the composite such as cracks and porosity that provide crucial in-service properties. It is considered more appropriate to assess the dynamic modulus of elasticity in case of dynamically loaded structures since it captures the full cycle of loading and relies fully on non-destructive approaches [10]. The non-linear nature of concrete arises from discontinuities within the material such as micro-pores and cracks. Concrete embedded reinforcements and sensors of different sizes increase the potential of discontinuities within a concrete structure. These affect the dynamic response of concrete in relation to its microstructure. Generally, the (E_d) is obtained using sonic vibration techniques that are mainly non-destructive in nature. Some Non-destructive Testing (NDT) methods rely on determining concrete properties using surface hardness or wave propagation properties. Currently, NDTs for measuring the dynamic elastic modulus of concrete depend on methods that entail stress wave propagation properties such as wave velocity and resonant frequency. Structural damage evaluation using non-destructive resonant frequency testing has reached considerable attention in recent years. The natural frequency is considered a reliable property that indicates the strength and durability of a structure. In addition, it is directly affected by significant deterioration and cracks within the structure. Any change directly related to the mass, stiffness or damping properties of the structure will lead to changes in the dynamic elastic properties such as the resonant frequencies, mode shapes and damping loss factors [11].

A great number of studies have been conducted on using the Resonance Frequency Testing (RFT) method to evaluate self-healing of plain concrete [12–19], but few experiments have been conducted on using this technique to measure the dynamic moduli of Fiber Reinforced Concrete (FRC) considering evaluation of induced cracks and self-healing efficiency [5]. For instance, recovery of the resonant frequency tested as a function of the crack width, reported by Li and Yang [5], showed that crack widths below 50 microns can recover up to 100% of its original resonant frequency when exposing cracked concrete to wet-dry cycle. As crack widths increase, concretes self-healing capability and resonant frequency recovery decreases. As the crack widths increase above 150 microns, Li and Yang reported that the resonant frequency remains unchanged after a wet-dry cycle to originate self-healing of concrete using Polyvinyl Acetate (PVA) [5]. The objective of the current study is to investigate the dynamic elastic properties of PFRC in concurrent evaluation of induced cracks and healing capability, using a non-destructive method that can be applied in monitoring the integrity of concrete structures. Also, this study aims to highlight the effects of polypropylene fibers on the dynamic properties of concrete prior/post crack induction, and post self-healing of cracks. Ultimately, results from this study will contribute in assessing the performance of existing and new PFRC structures to provide guidelines for structural designers and field examiners.

2. Experimental Program

2.1. Materials

Portland cement Type General Use (GU) (Canadian Standards Association (CSA) A23.1) was used for all concrete batches. In accordance with ASTM C150, this was Type 1 general use. Natural gravel with a nominal size of 12.5 mm containing a small amount of partially crushed material was used as coarse aggregates for all mixtures. Sand collected from Sechelt Pit was also used as fine aggregate. Table 1 includes the properties of the used aggregates.

Table 1. Coarse and fine aggregate properties.

Aggregate	Coarse	Fine
Maximum Size (mm)	12.5	4.75
Specific Gravity	2.8	2.7
Water Absorption (%)	0.45	1.2
Fineness	-	2.61

Two different polypropylene fibers were considered in this study developed by Propex Inc., Chattanooga, TN, USA. First is Type A (Enduro® 600), which is a macro-monofilament fiber with a patented sinusoidal deformation. Second is Type B (FiberMesh® 150), which is a 100% virgin polypropylene micro fiber. Table 2 includes the fiber material properties. Type A and Type B fibers used in this study are shown in Figure 2. Types A and B from here on in this study refer to designations for the macro and micro fibers respectively.

Table 2. Polypropylene Fiber Properties.

Mechanical Property	Unit	Type A Macro Polypropylene Fiber	Type B Micro Polypropylene Fiber
Fiber Length	mm	50	12
Equivalent Diameter	mm	0.5	0.018
Specific Gravity	-	0.91	0.9
Aspect Ratio	%	0.5	0.5
Elastic Modulus	GPa	7.5	7
Tensile Strength	MPa	550	300–450
Water Absorption	%	0	0
Melting Point	°C	164	162
Thermal Conductivity	W/mK	Low	N/A
Density	kg/m^3	910	900

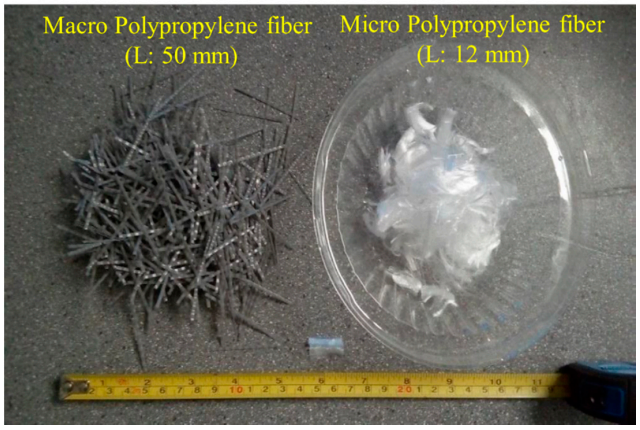

Figure 2. Macro (left) and micro (right) polypropylene fibers.

Potable clean tap water at 15 °C was used for all concrete mixtures. For the admixtures:

Water-Reducing Admixture (WRA)

MasterPozzolith 210 provided by BASF® (Victoria, BC, Canada) was used as the superplasticizer for mixtures. WRA was added to allow easier workability when adding fibers. A summary of the physical and chemical properties of WRA and AEA (discussed next) is provided in Table 3. The volume per 1 m^3 of WRA used for each batch is shown in Table 4.

Air-Entraining Admixtures (AEA)

Darex® Air-Entraining Admixtures (AEA) provided by Grace Canada, Inc. (Victoria, BC, Canada) was used as active air-entrainment during fresh concrete mixing. The admixture is an alkyl sulfate liquid composed essentially of tall oil. Tall oil is a by-product of chemical pulping of coniferous trees, such as pine trees, and is fundamentally made of fatty acids and another alkyl hydrocarbon derivates. AEA was added to supply concrete with microscopic air bubbles that protect the concrete through freeze-thaw cycles.

Table 3. Summary of admixture properties.

Item	Water-Reducing-Admixture (WRA)	Air-Entraining-Admixtures (AEA)
Supplier	BASF Canada, Inc.	Grace Canada, Inc.
Trade Name	POZZOLITH 210	DAREX AEA ED
Form	Liquid	Liquid, Oil-based
Color	Dark brown	Light brown
pH	6–11	11
Density (kg/m^3)	1125–1155	1000
Solubility in water	Completely soluble	
Solubility in other solvents		

2.2. Mixture Proportioning

The following mixture proportions were applicable for moderate to high strength concrete 31–45 MPa (Table 4). According to AASHTO-AGC-ARTBA Joint Committee, it is advised to increase the mortar fraction and reduce the coarse aggregate content to accommodate the increase in surface area due to polypropylene fiber addition [20].

Table 4. Mixture Proportions for Concrete.

Concrete Type	Type A	Type B
Fiber type	0.6% Macro PP	0.3% Micro PP
Mixture ID	MAC_PFRC	MIC_PFRC
w/c ratio	0.43	
Materials (kg/m^3)		
Cement	345	
Sand	815	
Aggregate	1045	
Water	145	
Fibers (% by volume)	0.6	0.3
Fibers	0.17	0.09
WRA	1.225	
AEA	0.123	

FRC comprises polypropylene fiber reinforced concrete with macro and micro fibers designated as A and B correspondingly for all batches. After several trial mixes with fiber content increasing to 1%, the fiber content with the highest flexural strength was chosen as 0.6% for macro fibers. On the other hand, a low fiber content of micro fibers was used since they exhibit a higher adsorption

capacity [21]. Fiber mixtures were regulated by modifying the quantity of WRA used while all AEA volumes remained constant between each batch. WRA dosages were adjusted to accommodate for low workability of fiber mixtures and maintain slump between all batches.

2.3. Specimen Preparation

The cylinders are cast according to ASTM C192 [22]. Each of the cylindrical molds (Ø100 × 200 mm) was cast in two layers. A total of 12 for measuring dynamic moduli and 6 for determination of compressive strength molds were prepared. Promptly after the casting, the specimens were sealed with a plastic sheet to maintain moisture for 24 h at room temperature during concrete hardening. After 24 h of hardening, cylinders were removed from the molds and saturated in a water bath set at 23 ± 2 °C for 28 days of curing [22]. For dry curing, conditions to see the effect of moisture content, samples were kept uncovered at ambient room temperature of 22 ± 2 °C at relative humidity of 50 ± 2%.

2.4. Testing

2.4.1. Fresh Concrete Properties

Workability of fresh concrete was measured using a slump test in accordance with ASTM C143 [23]. All mixtures were tested using the same apparatus and results are averaged to the nearest 5 mm. Air content is defined by the percentage of air present in a fresh concrete mixture. From ASTM C231, a Type B air meter was used for testing the percentage air in FRC mixtures as concrete the mixtures consist of relatively dense aggregates [24]. Air content testing was repeated twice to ensure consistent values. The density of a fresh concrete batch is measured in accordance with ASTM C138 and it is theoretically defined as the mass to volume ratio [25] For measuring fresh mixture density, a container of known volume and weight is filled to the brim with the freshly prepared concrete mixture. The fresh mixture was rodded to compensate the possibility of excessive loss in entrained air [25]. Temperature of fresh concrete mixture was measured in accordance with ASTM C1064 [26]. A thermometer was placed in different location of the mixture after the mixing process is complete and average reading of the temperature is reported.

2.4.2. Hardened Concrete Properties

Compressive Strength

In this study, cylindrical specimens Ø100 × 200 mm are compressed along their longitudinal axis. Each cylinder side was surface ground using a diamond grit-grinding disc having about 2 mm cut-off per side. This ensures even distribution of the load applied on the cylinder surface. All cylinders were tested according to ASTM C39 "Standard Test Method for Compressive Strength of Cylindrical Concrete Specimens" [27]. A Forney compression machine was used in this study that had a maximum capacity of 3000 KN with an applied loading rate maintained at 0.25 MPa/s for every test. The cylinders were saturated surface dry before each test. An average of 3-cylinder compression tests were used.

Resonant Frequency Testing

Impact resonant frequency testing was performed in accordance with ASTM C215 Standard test method for fundamental transverse, longitudinal and torsional resonant frequencies of concrete specimens [9] (Figure 3a). Although ASTM C215 states that this technique is for concrete specimens, the testing procedure could be carried out on paste and mortar specimens correspondingly. All cylindrical specimens were tested in the transverse and longitudinal modes of vibration. Although it is achievable to test the torsional mode of a cylinder with a 90° tab to align the accelerometer perpendicular to the curved surface, the curved surface of the cylinder and small aspect ratio makes it challenging to separate the torsional fundamental frequency from the transverse mode of excitation. For transverse vibration, the impact is released at center of the sample parallel to the accelerometer placed on the same

surface to simulate a simply supported bar. For longitudinal vibration, the setup was established by positioning the cylinders at a center node support (0.5L) with the accelerometer being perpendicular to the longitudinal impact direction. For nodal support, Neoprene bars 150 × 25 × 8 mm length, width, and thickness respectively were used as nodal supports. Figure 3c shows the cylindrical setup for the transverse mode of vibration.

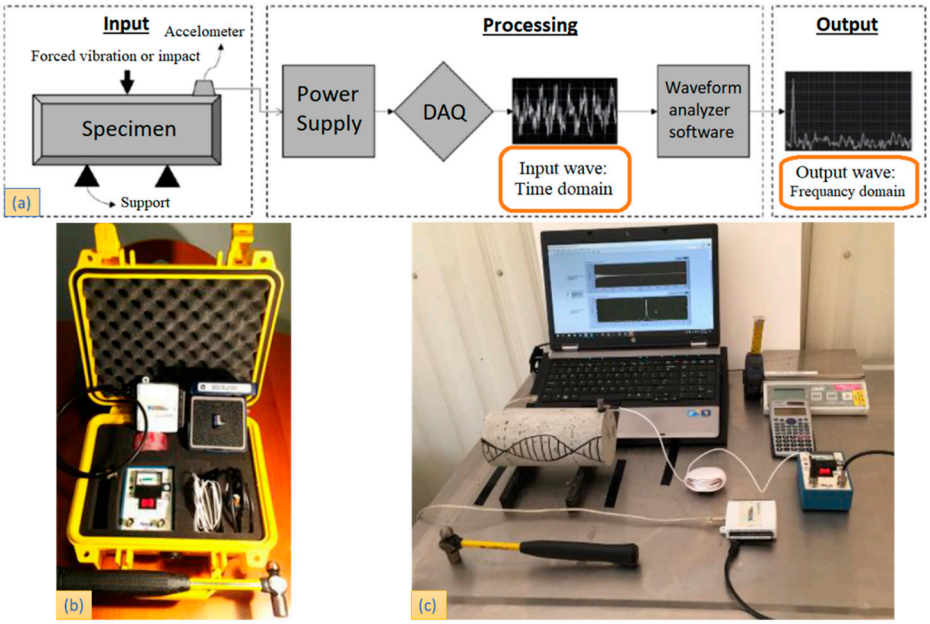

Figure 3. (**a**) Resonant Frequency Testing using Impact Method (**b**) Resonance Frequency Testing Equipment (**c**) Setup for cylindrical specimen (Transverse mode) (Adopted from [18]).

A Printed Circuit Board (PCB) Integrated Circuit Piezoelectric (ICP©) accelerometer (PCB group, Depew, NY, USA), with a pickup sensitivity of 102.2 mV/g (10.2 mV/ms^{-2}), and frequency range of 0.3–15 kHz, is attached to the concrete surface using microcrystalline adhesive wax. The accelerometer Model 352C33 was manufactured by PCB electronics. The attained time domain signal was amplified and passed through a low pass filter cut-off frequency at 10 kHz. The input compression wave voltage is collected using a 4 channel NI USB6009 DAQ (National Instruments, Vancouver, BC, Canada) with a built in Analog to Digital Convertor (ADC). After attaching the accelerometer and positioning the concrete samples to the required mode of testing, a standard ball tip hammer weighing 110 ± 2 g with a tip diameter of 10 mm, is used to strike the surface at precise locations on the samples being tested.

The Fast Fourier Transform (FFT) requirements are modeled in a visual instrument (VI) program using National Instrument's LabVIEW 2014 (NI LabVIEW) (National Instrument, Austin, TX, USA). The program was exclusively developed for this study considering ASTM C215 for acquisition requirements. Exponential windowing and averaging, along with a discrete frequency domain, were examined to ensure output noise reduction and coherence. All waveform acceleration responses were digitized in the time domain to 1024 samples at a sampling acquisition rate of 20 kHz. The sampling rate of a data acquisition system should be large enough for determining the highest predicted frequency to fulfill the Nyquist frequency. This led to a signal response time of 51.2 ms along with a sample interval (SI) of 25 µs. The spectral line spacing in the frequency domain, or digital step, is 19.5 Hz and the Nyquist frequency for the response is 10 kHz.

From the output amplitude-frequency graph, the first amplitude peak value verifies the natural resonant frequency according to the tested mode of vibration. The RFT tests were performed three times and averaged for all modes of vibration for each specimen. Any results deviating 10% from the mean frequency are disregarded and the test was repeated. Dynamic elastic moduli are calculated according to the equations of transverse and longitudinal modes of vibration using impact resonant

frequency testing in ASTM C215 [9]. The dynamic elastic moduli are determined through the following standard equations in Table 5 where m is the mass in kg, L is the cylinder length in meters, d is the cylinder diameter in meters, n is the fundamental transverse frequency in Hz and $n\prime$ is the fundamental longitudinal frequency in Hz.

Table 5. Governing equations for dynamic elastic moduli.

Mode	Equation	Cylinder Dimensional Factor
Transverse	$E_{dt} = Cmn^2$	$C = 1.6067\frac{L^3T}{d^4}$
Longitudinal	$E_{dl} = Dmn'^2$	$D = 5.093\frac{L}{d^2}$

Note that a correction factor T is used for calculation of the dynamic modulus of elasticity through transverse mode of vibration. This correction factor relies on the ratio between the radius of gyration (k) and length of the cylinder (L) given as $\left(\frac{K}{L}\right)$. A table included in ASTM C215 correlates this ratio with predetermined Poisson's ratio to provide the correction factor (T). For this study, a commonly presumed Poisson's ratio of 0.17 and a calculated correction factor of 2.11 was used for the calculation of the transverse dynamic modulus of elasticity.

For all cases, the specimen orientation was kept constant during testing to ensure that any changes observed in the specimen vibration response would not arise from changing the testing setup. Transverse vibration was carried out perpendicular to the direction of casting for all concrete cylinders. This was maintained to ensure that the dominant vibrational thickness is accounted for in the longitudinal vibration of cylinders. When testing concrete through multiple impacts, the surface may crumble. For reliable practice suggested by Malhotra and Carino [12] consecutive readings are measured at the same contact location of the hammer on the concrete surface and omitting the first two readings from the measured set to remove anomalies. The mode of vibration and equivalent resonant frequency for each mode are reported to nearest 10 Hz while the dynamic modulus of elasticity is calculated to the nearest 0.5 GPa.

Using ASTM C215 has been reported to be a promising technique for testing the extent and rate of autogenous healing of concrete [5]. Moreover, the standard, specifically referenced in ASTM C666 [28], appears to have a reliable indication in monitoring concrete degradation due to freeze and thaw cycles. Li and Yang [5] verified the validity of using resonant frequency testing as a measurement of internal concrete damage and healing through a series of frequency measurements on concrete prisms subjected to varying levels of strain deformation from 0% to 4% under uniaxial tension. The authors concluded that the measurement of resonant frequencies is capable of quantifying the degree of damage, with tensile strain beyond the first crack, and the rate of self-healing with respect to different exposures of wet-dry cycles.

2.4.3. Standard Crack Inducing Jig (SCIJ)

Figure 4a,b shows the Standard Crack Inducing Jig (SCIJ) developed by Gupta and Biparva [29]. This jig houses a Ø100 × 200 mm cylinder between v-shaped cutting edges that act as stress concentrators. Ideally, the SCIJ develops cracks ranging 0.1–0.5 mm in width. For achieving a consistent crack, the authors recommended that the ideal age to induce cracks is between 2–3 days of curing. This is due to the fact that that at earlier age (e.g., 1 day of curing), the concrete fractures in a ductile manner. While at later ages (e.g., 28 days of curing), the crack fracture behaves in a brittle manner. However, it is recommended by the authors to investigate the each mixture by cracking sample cylinders to ensure a consistent generated crack width. Hence, the aim of this study is to investigate the recovered dynamic moduli of macro and micro PFRC during two curing regimes prior to crack induction. For constant testing, the uniaxial tension is terminated as the concrete cylinder cracks for maintaining a constant crack width. With pilot investigation of the suggested cracks for the concrete mixture of this study, cylinders were cracked at 14 days.

The crack generated by the SCIJ should be measured from each face of the concrete cylinder. An average of five readings of the crack width were taken for each sample. After cracking the cylinder, the RFT was carried out again, in transverse mode, having the impulse direction perpendicular to the indentation from the SCIJ line to capture the full plane of cracking. Subsequently, the cracked PFRC cylinder was tested in the longitudinal mode as shown in Figure 4c. Since the crack area is along the longitudinal dimension of the cylinders, the expected longitudinal vibration may be inconsistent to interpret in the frequency domain. The longitudinal vibration was conducted as close to the center below the crack. By that, the longitudinal frequency variation may not indicate a notable change. All cracked cylinders are positioned in the same orientation for transverse and longitudinal testing. During testing, signal variations can occur due to external vibration, insecurely supported cables, or by disturbance in the accelerometer. After three strikes, any frequency measurements that deviated by 10% from the average value were disregarded and the test was repeated.

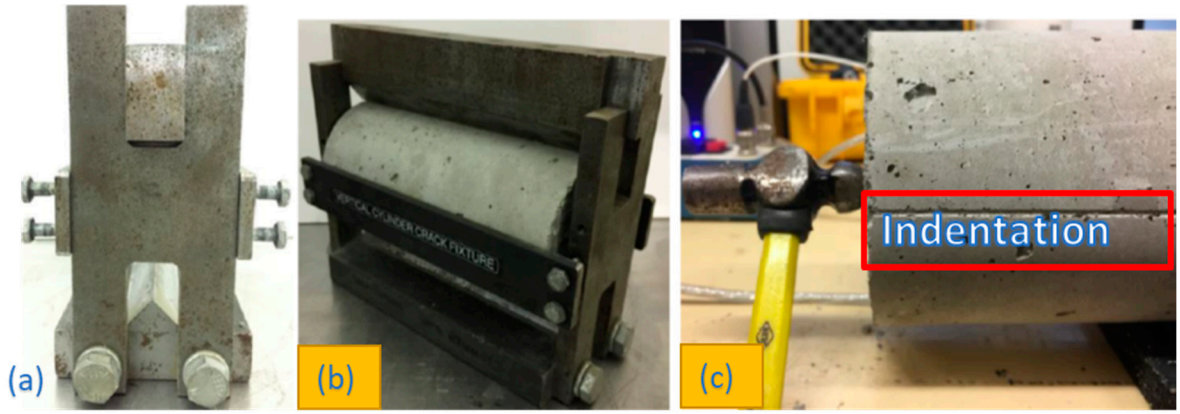

Figure 4. Setup for cracking (**a**) Standard Crack Inducing Jig (SCIJ) Front view (**b**) cylinder held in SCIJ Isometric view (**c**) Longitudinal Impulse Direction Setup.

3. Results and Discussion

3.1. Standard PFRC Properties

Workability of all concrete mixtures are defined using the slump test according to ASTM C143 [23] and summarized in Table 6. All fiber reinforced concretes are within the required slump range 115 ± 5 mm. In comparison to plain concrete mixtures, generally the slump decreases significantly when fibers are added to concrete during mixing. As the fiber volume increases, the deformability of a fresh FRC mixture decreases irrespective of the type. A low slump value is common for FRC, when compared to plain mixtures of the same mixture having the volume fraction of fibers as the dominant variable [30]. Fresh FRC mixtures with polypropylene micro fibers exhibited a lower slump than that of macro fibers. When added to a fresh concrete mixture, microfibers decrease the free available water content for the paste thus decreasing the workability. Microfibers decrease concretes' workability due the large surface area available for retaining (adsorbing) water while fibers have hydrophobic nature. Hence, a percentage of 0.3% micro fiber was used, when compared to 0.6% macro fibers. On the other hand, concrete containing polypropylene macro fibers was harder to consolidate and finish within the molds. As practiced in industry, WRA values were increased as the fiber content increases to maintain regular workability.

The air content was measured as an approach to detect any unbalanced air distribution. Improper air distribution in the mixture could result in production stage errors or defects during service period. The resulting air content of all batches are between 5–7% in accordance with ASTM C231 [24], as reported in Table 6. Density values are within the standard range of normal-weight concrete 2200–2400 kg/m^3 in accordance with ASTM C138 [25] reported in Table 6. It was observed

that an increase in the air content decreased the concrete density when fibers were added. This can be explained by the increase in porosity when fibers were added. Mixture temperature for all batches is tested in Winter in agreement with ASTM C1064 [26] and the average values were between 9–10 °C, as summarized in Table 6.

Compressive strength of concrete cylinders from each mixture were measured according to ASTM C39 [27]. Inclusion of both macro and micro polypropylene fibers had no substantial effect on concrete compressive strength. Addition of fibers marginally decreased the compressive strength compared to the plain concrete. The reduction increases when the volume fraction of fibers increases. Table 6 outlines the average compressive strength of both mixtures at 28 days from casting.

Table 6. Standard properties of fresh and hardened concrete.

Fresh Concrete Properties	Polypropylene Fiber Reinforced Concrete Type		Reference
	A **0.6% Macro Fiber**	**B** **0.3% Micro Fiber**	
Slump (mm)	120	110	ASTM C143
Air Content (%)	6.6	5.8	ASTM C231
Density (kg/m^3)	2216	2267	ASTM C138
Temperature (°C)	9.2	9.8	ASTM C1064
Hardened Concrete Properties	A 0.6% Macro Fiber	B 0.3% Micro Fiber	Reference
Compressive strength * (MPa)	31.55	34.91	ASTM C39

* Average of three readings tested at 28 Days on PFRC control specimens cured at 24 ± 2 °C.

3.2. Resonant Frequency and Dynamic Elastic Properties

The healing efficiency of concrete cylinders containing micro and macro PP fibers when adding polypropylene micro and macro fibers was studied. This was monitored by recording the frequency response of concrete when cracks are induced and then cured under wet and dry curing conditions. The resonant frequencies for concrete cylinders of three batches were evaluated using the IRM discussed in Section 2.4.2. Tests were conducted according to ASTM C215 [9]. Resonant frequency results were measured to the nearest 10 Hz as per the standard. Although this study includes lab-developed samples that are tested using low impact excitation at higher frequencies, recognizing minimal frequency variation for any given sample was achievable. Some limitations arise from both averaging and resolution of frequency since there is a finite number of samples, or bins, to generate the frequency domain.

Table 7 shows the first mode fundamental resonant frequencies of cylindrical specimens in this study when the transverse and longitudinal mode of vibration were tested at 14 days, prior/post cracking, and at 28 days after curing cracked samples in water. No crack closure was observed on dry specimens after 28-day exposure; thus, the frequency test for self-healing was not conducted on dry PFRC specimens. It was expected that autogenous self-healing will not take place as water is not present to activate the healing process. It is well known that constant presence of water is essential to activate and maintain the natural self-healing of cracked concrete [4].

From Table 7, it can be established that micro fiber PFRC exhibited higher resonant frequencies than that of macro fibers PFRC when comparing the original cylinders. Since micro fibers have a high adsorption capacity than that of macro fibers, curing of the PFRC specimen was more prominent when using micro fibers of the same water to cement ratio. With the same mix design, dry-cured PFRC exhibited ~200 Hz lower resonant frequencies than that of water-cured PFRC samples for both macro and micro fibers. For better visualization, data presented in Table 7 also plotted in Figure 5. Moreover, the authors believe that the longitudinal frequencies of self-healed cylinders are higher than there references due to further curing and hydration to 28 days. It is hypothesized that since the specimens were tested with RFT method at 14 days and then cracked, complete hydration of the

specimens has not yet been achieved. Hence, due to its high content of un-hydrated cement particles, when they were examined after 28 days wet-curing to determine recovery of dynamic elastic moduli, ongoing hydration was being take place and helped cylinders to attain higher longitudinal frequencies than their references.

By developing cracks in the cylinders, outlined in Section 2.4.3, both polypropylene macro and micro fibers effectively restrained crack propagation with macro fibers having a better performance in crack width closure. Keep crack widths consistent below 0.05 mm for ensuring that a full recovery can be attained is quite challenging. However, when using fibers, the self-healing of larger crack widths can still be achievable. Although crack widths of the cylindrical specimen used in this study are between 0.10–0.5 mm, partial recovery was observed. The regain in dynamic elastic properties post cracking illustrates the ductility of PFRC composites. An illustration of the frequency recovery is shown in Figures 6–8, which indicate the detected transverse vibration and the resulting resonant frequency of the original, cracked and self-healed water-cured micro fiber PFRC cylinder. The measured original transverse resonant frequency, post-cracking and self-healed frequencies are 5.91 kHz, 4.07 kHz and 4.23 kHz respectively.

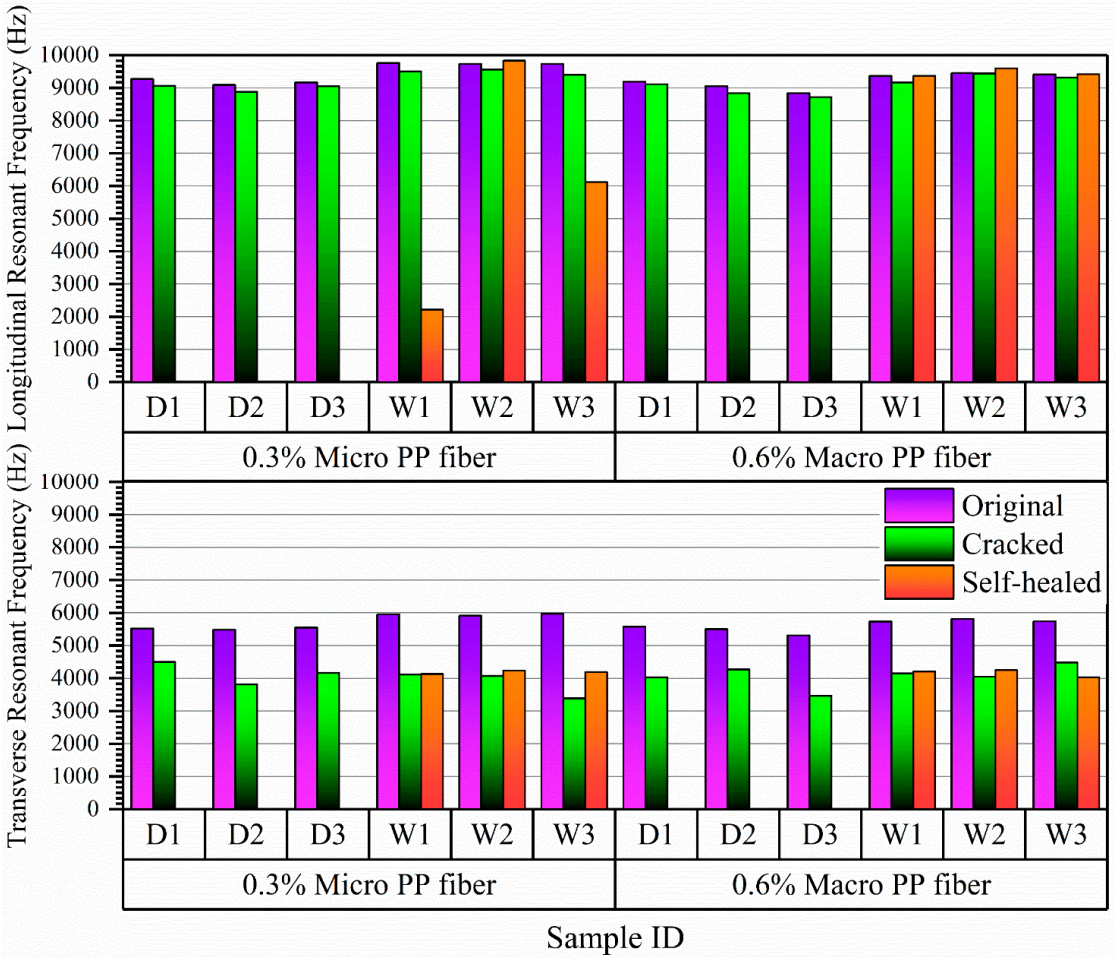

Figure 5. Frequency response of original, cracked and self-healed Polypropylene Fiber Reinforced Concrete (PFRC) samples.

Table 7. Transverse and longitudinal resonant frequency of PFRC specimens.

PFRC Sample ID	Fiber Type	Curing Condition	Measured Cylinder Mass (kg)	Transverse Mode			Longitudinal Mode		
				Original Frequency (Hz)	Cracked Frequency (Hz)	Self-Healing Frequency (Hz)	Original Frequency (Hz)	Cracked Frequency (Hz)	Self-Healing Frequency (Hz)
Mac-W1	Macro 0.6% (A)	Wet	3.58	5730	4150	4210	9360	9170	9370
Mac-W2			3.55	5810	4050	4250	9450	9440	9600
Mac-W3			3.55	5740	4480	4030	9410	9310	9420
Mac-D1		Dry	3.56	5580	4030	-	9190	9110	-
Mac-D2			3.55	5500	4270	-	9050	8840	-
Mac-D3			3.51	5310	3470	-	8840	8720	-
Mic-W1	Micro 0.3% (B)	Wet	3.69	5950	4110	4130	9760	9500	2220 [1]
Mic-W2			3.69	5910	4070	4230	9740	9560	9830
Mic-W3			3.67	5970	3390	4190	9740	9400	6120 [2]
Mic-D1		Dry	3.58	5520	4500	-	9270	9060	-
Mic-D2			3.55	5480	3820	-	9090	8880	-
Mic-D3			3.56	5550	4170	-	9170	9050	-

[1] Frequency peaks detected at ~9.25 KHz and ~9.75 KHz with 2.22 KHz being the highest peak; [2] Frequency peaks detected at ~2.50 KHz, 4.25 KHz and 5.75 KHz with 6.12 KHz being the highest peak.

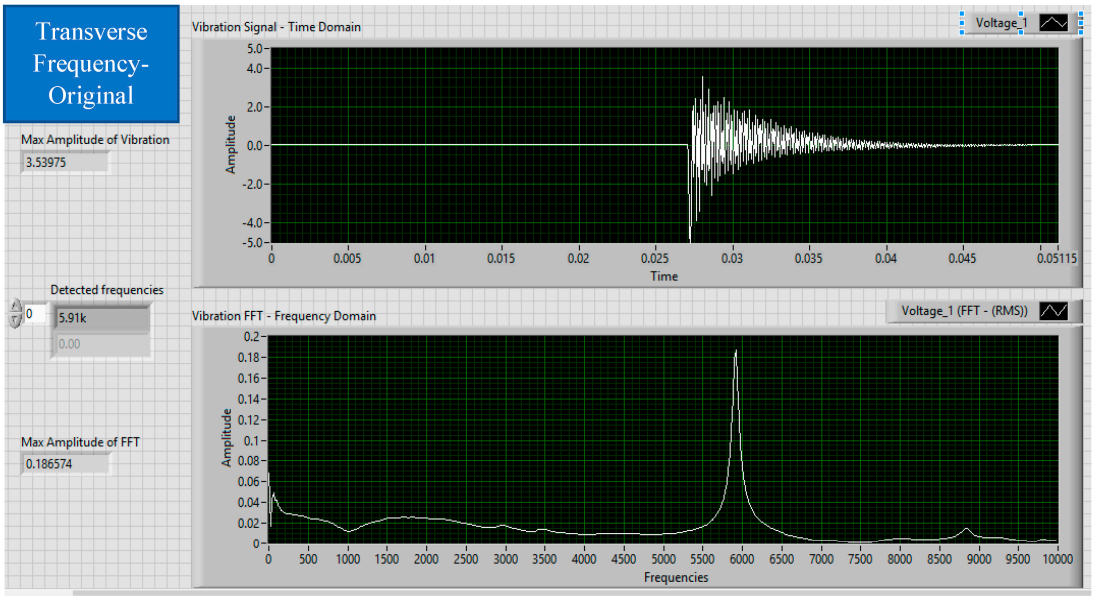

Figure 6. Transverse mode vibration and resonant frequency of original (uncracked) micro PFRC cylinder.

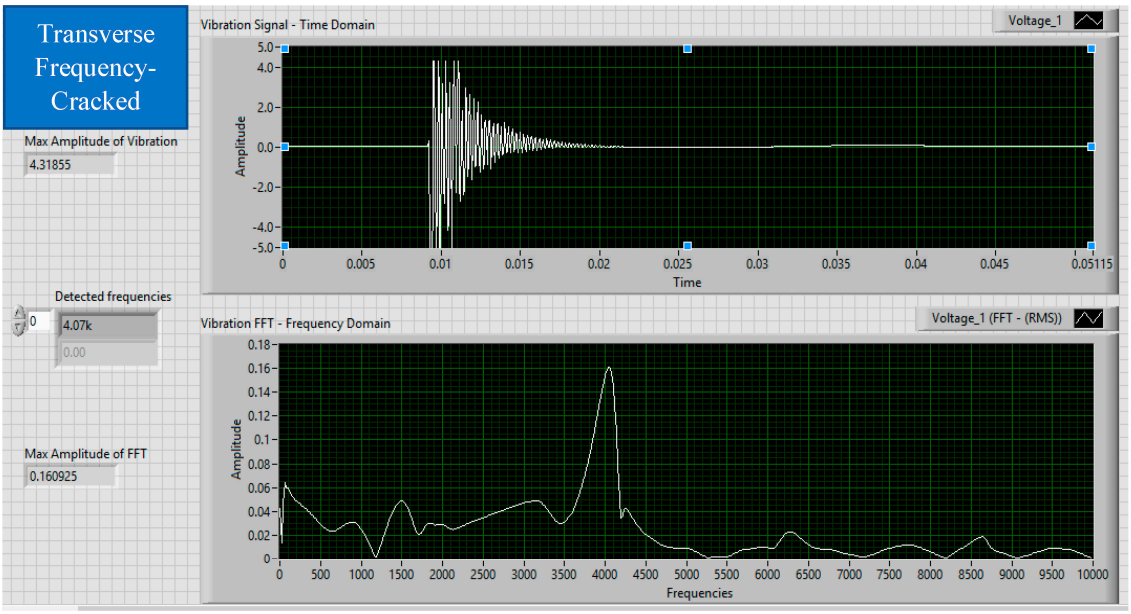

Figure 7. Transverse mode vibration and resonant frequency of cracked micro PFRC cylinder.

The dynamic modulus of elasticity was calculated from the obtained resonant frequencies. It was used to monitor the extent of self-healing of PFRC cylinders. All measurements are conducted on unloaded concrete cylinders cured in a water bath prior and post cracking. Variation in the frequency between samples of the same mixture can be a product of difference in a length and frequency resolution. Hence, the dynamic modulus of elasticity was calculated to account for the variation in cylinder mass and length. Since the dynamic modulus of elasticity is proportional to the resonant frequency keeping other factors constant, the moduli results are expected to follow the same trend as that of the frequency while accounting for dimensional factors. Table 8 shows the calculated transverse and longitudinal dynamic elastic moduli of water-cured PFRC cylinders. Note that the self-healed

results for micro PP-W1 and micro PP-W3 of the longitudinal mode of vibration are only calculated for the detected maximum frequency thus may not provide a true indication of self-healing.

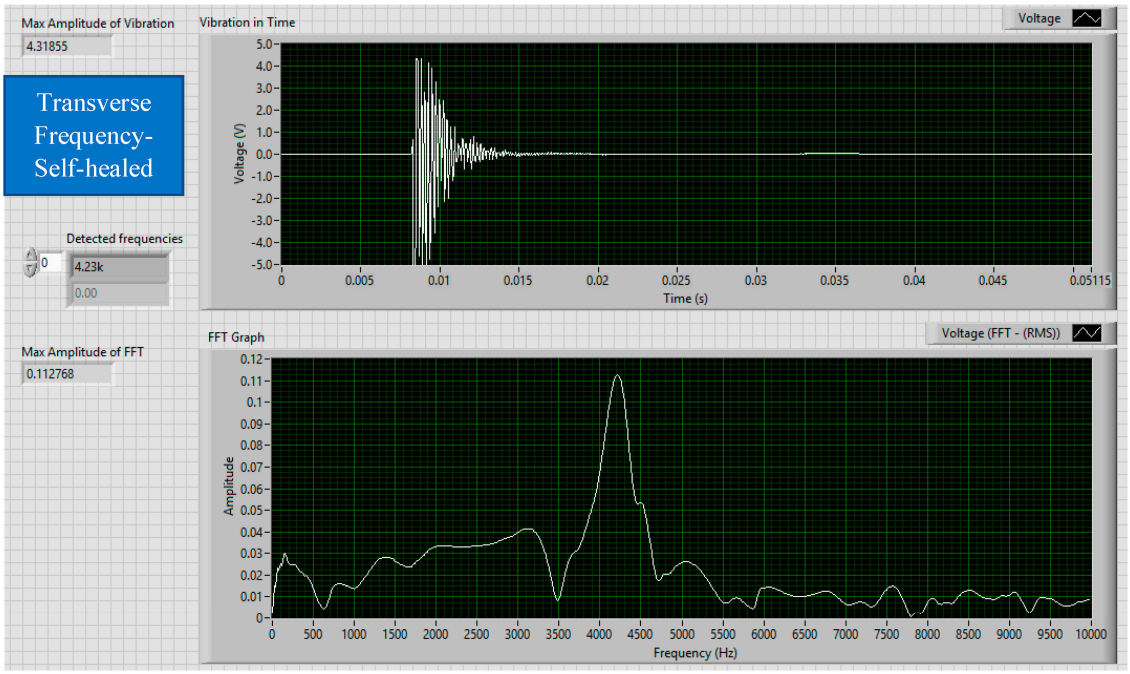

Figure 8. Transverse mode vibration and resonant frequency of self-healed micro PFRC cylinder.

Table 8. Dynamic modulus of elasticity of water-cured PFRC cylinders.

Dynamic Modulus of Elasticity (GPA)						
Mode	Transverse			Longitudinal		
FIBER TYPE	Original	Cracked	Self-Healed	Original	Cracked	Self-Healed
MACRO PP-W1	31.6	16.6	17.0	31.6	30.4	31.7
MACRO PP-W2	32.2	15.6	17.2	32.0	31.9	33.0
MACRO PP-W3	31.4	19.1	15.5	31.7	31.0	31.8
MICRO PP-W1	35.1	16.7	16.9	35.4	33.6	1.8
MICRO PP-W2	34.6	16.4	17.7	35.3	34.0	36.0
MICRO PP-W3	35.1	11.3	17.3	35.1	32.7	13.9

Figure 9 shows the calculated dynamic moduli of PFRC cylinders in transverse and longitudinal modes as a function of crack width. The graph provides the dynamic elastic modulus of cracked and self-healed cylinders averaged from three impacts per cylinder during RFT and normalized to the original (un-cracked) elastic modulus of PFRC cylinders. The results indicated that the fiber size affects the extent and recovery of the PFRC elastic modulus. Macro fibers were more effective in recovering the elastic properties in the longitudinal mode of vibration than micro fibers. On the other hand, micro fibers were more effective in transverse mode elastic recovery. Conversely, the larger fiber size of macro fibers provides a good indication of recovery by bridging larger cracks.

Dynamic moduli values for cracked and self-healed PFRC samples were normalized to original modulus and represent as function of crack width in Table 9. According to the study conducted by Li and Yang [5], when a crack width exceeds 0.15 mm, it is considered difficult to repair microstructural damage of cracks and thus frequency recovery is not expected. Therefore, it was recommended by the authors to maintain a crack width below 0.15 mm and preferably below 0.05 mm to maintain a full recovery. However, in the case of the PFRC cylinders cracked in this study, partial recovery was

achieved at cracks between 0.2 mm to 0.5 mm by using macro fibers indicating that self-healing can be achieved.

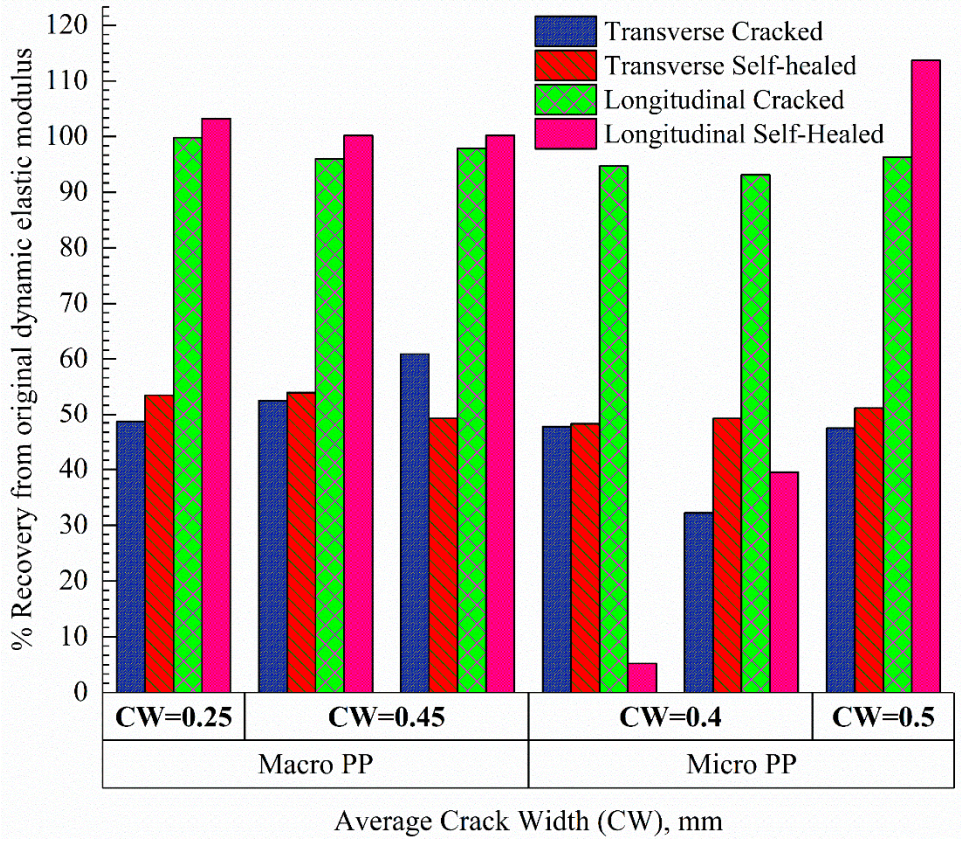

Figure 9. Recovery of dynamic elastic modulus in transverse and longitudinal mode as a function of crack width.

Table 9. Percentage of cracked and self-healed dynamic moduli, as a function of crack width, normalized to the original modulus.

Fiber Type	Crack Width (mm)	Transverse Cracked (%)	Transverse Self-Healed (%)	Longitudinal Cracked (%)	Longitudinal Self-Healed (%)
Macro PP-W1	0.45	52.5	54.0	96.0	100.2
Macro PP-W2	0.25	48.6	53.5	99.8	103.2
Macro PP-W3	0.45	60.9	49.3	97.9	100.2
Micro PP-W1	0.4	47.7	48.2	94.7	5.2
Micro PP-W2	0.5	47.4	51.2	96.3	113.7
Micro PP-W3	0.4	32.2	49.3	93.1	39.5

4. Conclusions

Healing capability and dynamic moduli recovery of polypropylene fiber reinforced concrete cylinders have been investigated using resonance frequency testing. Monitoring the resonant frequency of concrete cylinders using ASTM C215 appears to provide a reliable indication of both crack detection and self-healing (crack closure) of concrete. By using the calculated dynamic modulus of elasticity, which accounts for the specimen mass, length, and dimensional factors, the indication is apparent and can be used to assess the extent and rate of damage and self-healing of concrete. Both dynamic transverse and longitudinal moduli of elasticity were used to investigate the rate and extent of PFRC natural self-healing. Micro fibers exhibited higher percentage recovery of elasticity in transverse mode vibration while macro fibers exhibited higher percentage recovery in longitudinal mode. This can be a

result of the finer crack size bridged by micro fibers in transverse mode and the larger crack size that macro fibers subdue in longitudinal mode respectively. For additional research on the reproducibility of self-healing, the authors recommend using the longitudinal elastic modulus since it does not account for correction factors. However, care should be taken to position the vibrational support at the midspan of the concrete cylinder. Furthermore, it is expected that further hydration can contribute to a larger recovery and facilitate additional self-healing.

Authors recommend pursuing the correlation between cracked, un-cracked and self-healed concrete through the dynamic modulus of elasticity, instead of using the resonant frequency solely, since the latter accounts for specimen weight and dimensional factors. On-going work includes studying the effects of crystalline admixtures and bacteria incorporated with PFRC specimen. Effect of cracks' widths—in a wider range of 0.05 to 1.0 mm—on self-healing and recovery of dynamic moduli is also investigated. Examination of hybrid mix of macro- and micro-pp fibers is also part of authors' ongoing research, which will be reported in future.

Acknowledgments: The authors would like to acknowledge the contribution of Propex Inc. for their donation of the fibers used in this study.

Author Contributions: Adham El-newihy, Pejman Azarsa, Rishi Gupta and Alireza Biparva conceived and designed the experiments; Adham El-newihy and Pejman Azarsa performed the experiments; Adham El-newihy, Pejman Azarsa and Rishi Gupta analysed the data; Rishi Gupta and Alireza Biparva contributed materials and experimental equipment; Adham El-newihy, Pejman Azarsa and Rishi Gupta wrote the paper.

Conflicts of Interest: The authors declare no conflict of interest.

References

1. Cailleux, E.; Pollet, V. Investigations on the development of self-healing properties in protective coatings for concrete and repair mortars. In Proceedings of the 2nd International Conference on Self-Healing Materials, Chicago, IL, USA, 28 June–1 July 2009.
2. Yunovich, M.; Thompson, N.G. Corrosion of Highway Bridges: Economic Impact and Control Methodologies. *Concr. Int.* **2003**, *25*, 52–57.
3. Woudhuysen, J.; Abley, I. *Why is Construction so Backward?* Wiley-Academy: Chichester, UK; Hoboken, NJ, USA, 2004.
4. Van Tittelboom, K.; de Belie, N. Self-Healing in Cementitious Materials—A Review. *Materials* **2013**, *6*, 2182–2217. [CrossRef] [PubMed]
5. Li, V.C.; Yang, E.-H. Self-healing in concrete materials. In *Self-Healing Materials*; Springer: Berlin, Germany, 2007; pp. 161–193.
6. Ferreira, J.P.J.G.; Branco, F.A.B. The use of glass fiber–reinforced concrete as a structural material. *Exp. Tech.* **2007**, *31*, 64–73. [CrossRef]
7. Mu, R.; Miao, C.; Luo, X.; Sun, W. Interaction between loading, freeze–thaw cycles, and chloride salt attack of concrete with and without steel fiber reinforcement. *Cem. Concr. Res.* **2002**, *32*, 1061–1066. [CrossRef]
8. Naaman, A.; Namur, G.; Najm, H.; Alwan, J. *Bond Mechanisms in Fiber Reinforced Cement-Based Composites*; Michigan University Ann Arbor Department of Civil Engineering: Ann Arbor, MI, USA, 1989.
9. ASTM C215-14. *Standard Test Method for Fundamental Transverse, Longitudinal, and Torsional Resonant Frequencies of Concrete Specimens*; ASTM International: West Conshohocken, PA, USA, 2014.
10. Mindess, S.; Young, J.F.; Darwin, D. *Concrete*, 2nd ed.; Prentice Hall: Upper Saddle River, NJ, USA, 2003.
11. He, J. Damage Detection and Evaluation I. In *Modal Analysis and Testing*; Silva, J.M.M., Maia, N.M.M., Eds.; Springer: Dordrecht, The Netherlands, 1999; pp. 325–344.
12. Malhotra, V.M.; Carino, N.J. *Handbook on Nondestructive Testing of Concrete Second Edition*; CRC Press: Boca Raton, FL, USA, 2003.
13. Yang, Y.; Lepech, M.D.; Yang, E.-H.; Li, V.C. Autogenous healing of engineered cementitious composites under wet–dry cycles. *Cem. Concr. Res.* **2009**, *39*, 382–390. [CrossRef]
14. Jacobsen, S.; Sellevold, E.J. Self-healing of high strength concrete after deterioration by freeze/thaw. *Cem. Concr. Res.* **1996**, *26*, 55–62. [CrossRef]

15. Yang, Y.; Yang, E.-H.; Li, V.C. Autogenous healing of engineered cementitious composites at early age. *Cem. Concr. Res.* **2011**, *41*, 176–183. [CrossRef]
16. Abd_Elmoaty, A.E.M. Self-healing of polymer modified concrete. *Alex. Eng. J.* **2011**, *50*, 171–178. [CrossRef]
17. Sahmaran, M.L.M.; Li, V.C. Transport Properties of Engineered Cementitious Composites under Chloride Exposure. *ACI Mater. J.* **2007**, *104*, 604–611.
18. El-Newihy, A. Application of Impact Resonance Method for Evaluation of the Dynamic Elastic Properties of Polypropylene Fiber Reinforced Concrete. Master's Thesis, University of Victoria, Victoria, BC, Canada, 2017.
19. Azarsa, P.; Gupta, R. Electrical Resistivity of Concrete for Durability Evaluation: A Review. *Adv. Mater. Sci. Eng.* **2017**, *2017*, 8453095. [CrossRef]
20. AASHTO-AGC-ARTBA Joint Cooperation Committee. *The Use and State-of-the-Practice of Fiber Reinforced Concrete*; TF36-1-UL; American Association of State Highway and Transportation Officials: Washington, DC, USA, 2001.
21. Banthia, N.; Gupta, R. Influence of polypropylene fiber geometry on plastic shrinkage cracking in concrete. *Cem. Concr. Res.* **2006**, *36*, 1263–1267. [CrossRef]
22. ASTM C192/C192M-15. *Standard Practice for making and Curing Concrete Test Specimens in the Laboratory*; ASTM International: West Conshohocken, PA, USA, 2015.
23. ASTM C143/C143M-15a. *Standard Test Method for Slump of Hydraulic-Cement Concrete*; ASTM International: West Conshohocken, PA, USA, 2015.
24. ASTM C231/C231M-14. *Standard Test Method for Air Content of Freshly Mixed Concrete by the Pressure Method*; ASTM International: West Conshohocken, PA, USA, 2014.
25. ASTM C138/C138M-17a. *Standard Test Method for Density (Unit Weight), Yield, and Air Content (Gravimetric) of Concrete*; ASTM International: West Conshohocken, PA, USA, 2017.
26. ASTM C1064/C1064M-12. *Standard Test Method for Temperature of Freshly Mixed Hydraulic-Cement Concrete*; ASTM International: West Conshohocken, PA, USA, 2012.
27. ASTM C39/C39M-15a. *Standard Test Method for Compressive Strength of Cylindrical Concrete Specimens*; ASTM International: West Conshohocken, PA, USA, 2015.
28. ASTM C666/C666M-15. *Standard Test Method for Resistance of Concrete to Rapid Freezing and Thawing*; ASTM International: West Conshohocken, PA, USA, 2015.
29. Gupta, R.; Biparva, A. Innovative Test Technique to Evaluate 'Self-Sealing' of Concrete. *J. Test. Eval.* **2015**, *43*, 1091–1098. [CrossRef]
30. Kakooei, S.; Akil, H.M.; Jamshidi, M.; Rouhi, J. The effects of polypropylene fibers on the properties of reinforced concrete structures. *Constr. Build. Mater.* **2012**, *27*, 73–77. [CrossRef]